Biology of Reproduction, 2020, 103(1), 104–113
doi:10.1093/biolre/ioaa044
Research Article
Advance Access Publication Date: 14 April 2020

OXFORD

Research Article

Contribution of senescence in human endometrial stromal cells during proliferative phase to embryo receptivity†

Hiroyuki Tomari[1,2], Teruhiko Kawamura[1], Kazuo Asanoma[1], Katsuko Egashira[1], Keiko Kawamura[1], Ko Honjo[2], Yumi Nagata[2] and Kiyoko Kato[1,*]

[1]Department of Obstetrics and Gynecology, Graduate School of Medical Sciences, Kyushu University, Fukuoka, Japan and [2]Center for Reproductive Medicine, IVF Nagata Clinic, Fukuoka, Japan

***Correspondence**: Department of Obstetrics and Gynecology, Graduate School of Medical Sciences, Kyushu University, Maidashi 3-1-1, Higashi-ku, Fukuoka 812-8582, Japan. Tel: +81-92-642-5396; E-mail: kkato@med.kyushu-u.ac.jp

† **Grant Support**: This work was supported by Grants-in-Aid for Scientific Research on Innovative Areas "Stem Cell Aging and Disease" (JP15H01517) from the Ministry of Education, Culture, Sports, Science, and Technology (MEXT) (Japan) and Grants-in-Aid for Exploratory Research (JP18K19618) from MEXT (Japan) to K.K.

Received 26 October 2019; Revised 25 February 2020; Accepted 10 April 2020

Abstract

Successful assisted reproductive technology pregnancy depends on the viability of embryos and endometrial receptivity. However, the literature has neglected effects of the endometrial environment during the proliferative phase on implantation success or failure. Human endometrial stromal cells (hESCs) were isolated from endometrial tissues sampled at oocyte retrieval during the proliferative phase from women undergoing infertility treatment. Primary hESC cultures were used to investigate the relationship between stemness and senescence induction in this population and embryo receptivity. Patients were classified as *receptive* or *non-receptive* based on their pregnancy diagnosis after embryo transfer. Biomarkers of cellular senescence and somatic stem cells were compared between each sample. hESCs from non-receptive patients exhibited significantly higher ($P < 0.01$) proportions of senescent cells, mRNA expressions of *CDKN2A* and *CDKN1A* transcripts ($P < 0.01$), and expressions of genes encoding the senescence-associated secretory phenotype ($P < 0.05$). hESCs from receptive patients had significantly higher ($P < 0.01$) mRNA expressions of *ABCG2* and *ALDH1A1* transcripts. Our findings suggest that stemness is inversely associated with senescence induction in hESCs and, by extension, that implantation failure in infertility treatment may be attributable to a combination of senescence promotion and disruption of this maintenance function in this population during the proliferative phase of the menstrual cycle. This is a promising step towards potentially improving the embryo receptivity of endometrium. The specific mechanism by which implantation failure is prefigured by a loss of stemness among endometrial stem cells, and cellular senescence induction among hESCs, should be elucidated in detail in the future.

Summary sentence

Senescence induction and loss of stemness in human endometrial stromal cells during the proliferative phase are associated with embryo implantation failure.

Key words: human endometrial stromal cell, cellular senescence, endometrial stem cell, embryo receptivity, infertility.

Introduction

Assisted reproductive technology (ART) has made astounding progress in the 40 years since the first successful in vitro fertilization and embryo transfer (IVF/ET), including the development of other techniques such as ovulation induction, in vitro embryo culture, and cryopreservation. Despite these advances, live birth rates among ART-treated women currently remain low. It is known that ovarian function declines and oocyte aging due to maternal age increases, resulting in low pregnancy and high miscarriage rates [1]. Moreover, older women are at greater risk of producing aneuploid embryos, a correlation that has become apparent with the recent spread of preimplantation genetic testing for aneuploidy (PGT-A), especially in Europe and America [2]. Conversely, PGT-A can allow even older patients to achieve high pregnancy rates, comparable with their younger counterparts, by ensuring the embryos to be transferred have euploidy [2]. Thus, healthy, fertility oocytes and embryos are key to a successful live birth using ART. However, the clinical pregnancy rate resulting from ETs with confirmed euploidy by PGT-A is not 100%: It is closer to 50–70% [2–4]. This is because a successful ART pregnancy depends on the viability of the embryo and endometrial receptivity: the uterine lining's capacity to accept and attach embryos. Observations from IVF/PGT-A cycles suggest that endometrial dysfunction (decreased endometrial receptivity) is the cause of implantation failure in about 30% of cases.

Endometrial tissue undergoes regular physiological changes mediated by female sex hormones secreted by the ovaries during the menstrual cycle. Estradiol released during the proliferative phase thickens the endometrium. After ovulation, progesterone released during the secretory phase alters the form and function of hypertrophic endometrial stromal cells by a process called decidualization. Normal decidualization is essential to embryonic implantation by suppressing the mother's immune response to permit the infiltration of differentiated trophoblast cells [5, 6]. Decidualization has received major attention in the literature on endometrial receptivity, and steps involved in the normal process and how it can be suppressed by deleting critical genes to preclude pregnancy have been reported [7–11]. Notably, Ruiz-Alonso et al. [12] reported that an endometrial receptivity array (ERA)—genetic profiling and analysis of endometrial tissue sampled during a normal or hormone replacement therapy (HRT) cycle—effectively identified an appropriate implantation window. However, the literature has neglected the effects of the endometrial environment on implantation success and failure. In a previous study using healthy endometrium, we isolated and identified side population (SP) cells, a subset of cells in somatic tissues with stem cell-like properties (e.g., undifferentiated state, auto-renewal, multipotency) that are characterized by weak Hoechst 33342 uptake [13]. We also showed that the estrogen receptor (ER) was highly expressed in this population [14] and that this protein's functional inactivation induces cellular senescence via the p53/p21 signaling pathway [15]. Taken together, senescence in endometrial stem cells might limit the endometrium's ability to accommodate infiltration by embryonic and trophoblast cells. However, this possibility has not been reported. We hypothesized that disruption of the maintenance of endometrial stem cells could lead to cellular senescence of endometrial cells, resulting in decreased embryo receptivity and implantation failure.

In this study, we examined whether the expressions of senescence and stem cell marker genes and proteins in human endometrium stromal cells (hESCs) isolated from endometrium sampled during the proliferative phase of the menstrual cycle were associated with embryonic receptivity among women undergoing infertility treatment with IVF/ET.

Materials and methods

Ethics statement

Our study was conducted with the approval of the Clinical Research Ethics Review Committee of Kyushu University (approval number: 25–44).

Endometrial tissue collection

Our study was conducted with the approval of the Clinical Research Ethics Review Committee of Kyushu University. Human endometrial tissue was collected from 43 consenting patients undergoing infertility treatment at the IVF Nagata Clinic, during the oocyte retrieval step (age range: 28–45 years, Supplemental Table S1). A small amount of endometrial tissue was harvested from the anterior or posterior wall of the uterus under anesthesia using a Reicherschald biopsy curette (Atom Medical Corp., Saitama, Japan) and immediately washed with phosphate-buffered saline (PBS; Nakamedical Inc., Tokyo, Japan) (Supplemental Figure S1). Patient age, body mass index, endometrial thickness, and circulating estradiol (E2), progesterone (P4), luteinizing hormone (LH), and follicle-stimulating hormone (FSH) levels were recorded at the time of oocyte retrieval. Endometrial thickness was measured using transvaginal ultrasound (F37; Hitachi Aloka Medical, Tokyo, Japan), and each hormone was measured using an automated immunology analyzer (ARCHITECT*i*1000SR; Abbott Japan, Tokyo, Japan). Women then underwent IVF/ET according to a previously reported [16, 17] procedure. Briefly, ovarian stimulation was achieved by a short protocol using gonadotropin-releasing hormone agonist. Follicle growth was stimulated by injecting human menopausal gonadotropin (hMG, Gonapure; ASKA Pharmaceutical, Tokyo, Japan). In a few cycles, the minimal stimulation and natural cycle protocols were used. The minimal stimulation protocol was started with an extended regimen of clomiphene citrate in conjunction with low-dose gonadotropin injections. In the natural cycle protocol, the only pharmaceutical intervention involved the induction of final oocyte maturation. The ovarian response was monitored by daily measurement of follicle diameter. When at least one or two follicles had reached ≥18 mm in diameter, an injection of 10 000 IU of human chorionic gonadotropin (hCG; Fuji Pharma Co., Tokyo, Japan) was given intramuscularly

to mimic the normal LH surge. Oocytes were recovered 35–36 h after the administration of hCG following transvaginal ultrasound-guided puncture of the follicles. ET was performed using cleavage-stage embryos on day 2 during the same cycle as biopsy collection. Embryos that had reached the two-cell stage by 27 h post insemination and had good morphological scores (≥4 cells with <50% fragmentation) on day 2 were defined as good quality embryos. Successful implantation (i.e., pregnancy) was defined as circulating hCG levels of ≥20 mIU/ml at 2 weeks after ET. Based on the results of the hCG levels, patients with successful implantation were defined as receptive (n = 11) groups, and patients with implantation failure were defined as non-receptive (n = 32) groups (Supplemental Table S2). Grouping was performed using only the results of this study, regardless of the pregnancy and delivery histories prior to the study. Among the receptive group, six cycles were miscarriage and five cycles were ongoing pregnancy, which were confirmed by fetal heartbeat. We performed a cytogenetic analysis of products of conception and found that most of the causes of miscarriage after ART were due to embryo aneuploidy [unpublished data]. It is also known that the miscarriage rate is extremely low in euploid embryo transfer [2–4]. In other words, most miscarriage cases are likely to have normal embryo receptivity, so miscarriage cases were also defined as receptive group. In addition, a biopsy of endometrial tissue, oocyte retrieval, and embryo transfer was performed only once per patient.

Isolation of human endometrium stromal cells (hESCs)

hESCs were isolated using a slightly modified version of the procedure used by Satyaswaroop et al. [18] and Seli et al. [19]. Washed tissue was mechanically fragmented, immersed in 0.25% collagenase type I solution (Thermo Fisher Scientific, Inc., Waltham, MA, USA), and agitated for 2 h at 37 °C. The resulting cell suspension was filtered through a 35-μm cell strainer to separate epithelial and stromal cells (Falcon 352235; Corning Inc., Corning, NY, USA). Collagenase treatment disperses stromal cells, but not epithelial cells; the latter were caught by the nylon mesh, while hESCs passed through in the filtrate. Isolated cell identities were confirmed by subjecting a fraction of each sample to immunofluorescence staining following culture. Over 90% of cells were positive for the stromal cell marker vimentin and negative for the epithelial cell marker cytokeratin (Supplemental Figure S2).

Primary hESC cultures

Primary hESC cultures were established as described previously [13]. Cells were cultured in Dulbecco Modified Eagle medium (DMEM: Sigma Aldrich, St. Louis, MO, USA) supplemented with 20 μg/ml Gly-His-Lys (Sigma Aldrich), 4 μg/ml insulin (Thermo Fisher Scientific), 10% fetal bovine serum (FBS: Sigma Aldrich), and 1% penicillin/streptomycin (Thermo Fisher Scientific) at 37 °C under an atmosphere of 95% air and 5% CO_2. Cultures were passaged at 80% confluence. All experiments used first- or second-generation hESCs. Cells from passage 1 culture were used for hESC confirmation and total RNA extraction. Cells from passage 2 cultures were used for senescence-associated β-galactosidase (SA-β-Gal) staining and cell cycle analysis. Enzyme-linked immunosorbent assay (ELISA) was performed on supernatants from passage 2 cultures. Because of the small size of the endometrium samples, stromal cell counts for some women were too low to subject them to all tests. The specific tests performed on tissue from each subject are given in Supplemental Table S3.

SA-β-gal staining

β-galactosidase activity, specifically that of SA-β-gal, is enhanced in senescent cells at pH 6.0. In this study, X-Gal, a β-galactosidase that stains blue upon hydrolytic cleavage, was used to identify senescent cells.

Passage 2 hESCs were seeded in a 35-mm dish (Falcon; Corning Inc.) at a density of 3.0×10^4, and then stained at 2, 4, 6, and 8 days after inoculation. Cells were washed with PBS and then treated with a fixative solution containing PBS, 2% formaldehyde, and 0.2% glutaraldehyde for 5 min at room temperature. Next, after rewashing with slightly basic PBS, cells were incubated overnight at 37 °C under atmospheric air in SA-β-Gal staining solution (sodium phosphate [pH 6.0], 40 mM citric acid, 5 mM potassium ferricyanide, 5 mM potassium ferrocyanide, 150 mM NaCl, 2 mM $MgCl_2$, 1 mg/ml X-Gal). Senescence rate was defined as the ratio of blue (SA-β-Gal-positive) cells to total cells, counted visually after staining using a phase contrast microscope. Cell counts were collected by a third party blinded to sample information to minimize subjectivity.

Cell cycle analysis

Passage 2 hESCs were cultured for 8 days in a 100-mm dish (Falcon; Corning Inc.). Next, samples ≥1.0×10^6 cells were removed from the cell culture dish and fixed in 70% ethanol overnight at −20 °C. Samples were then centrifuged at 300 × g for 5 min, and the ethanol was removed. Next, the pellet was suspended in PBS containing 0.5% RNase and then incubated for 30 min at room temperature to digest the RNA. Then, 25 μm/ml propidium iodide was added, and the samples were incubated for 15 min on ice in a dark area to stain the DNA. Samples were passed through a 35-μm cell strainer (Corning Inc.) to remove cell aggregates. DNA content was measured for at least 20 000 cells using the BD FACSCalibur platform (BD Bioscience, Franklin Lakes, NJ, USA) according to the manufacturer's instructions. ModFit LT software was used for cell cycle analysis (Verity Software House, Topsham, MA, USA).

Quantitative real-time PCR (qRT-PCR)

Quantitative RT-PCR was used to quantify the expression of three senescence-associated (SA) genes (*CDKN2A*, *CDKN1A*, *TP53*; respectively encoding p16, p21, and p53), four genes belonging to the senescence-associated secretory phenotype (SASP: *IL6*, *CXCL8*, *IL17A*, *CCL2*), and two genes highly expressed in somatic stem cells (*ABCG2*, *ALDH1A1*). Total RNA was extracted from passage 1 hESCs (100 000 to 300 000 cells) using a RNeasy Mini Kit (Qiagen, Venlo, Netherlands) according to the manufacturer's protocol. RNA purity and concentration were measured using a NanoDrop ND-1000 spectrophotometer (NanoDrop Technologies Inc., Wilmington, DE, USA). cDNA was synthesized from extracted total RNA (200 ng) by reverse transcription using a ReverTra Ace kit (Toyobo, Osaka, Japan) according to the manufacturer's protocol. Random primers were used for the reverse transcription. Gene expression levels were investigated using the synthesized cDNA as a template and the respective gene-specific primers shown in Supplemental Table S4. Relative quantification of gene expression levels was performed using the Applied Biosystems 7500 Real-Time PCR System (Thermo Fisher Scientific) according to manufacturer's instructions using the ΔΔCt method [20]. The reaction mixture was subjected to an initial denaturation, followed by 40 PCR cycles (95 °C, 5 s; 60 °C, 34 s) using the SYBR Premix Ex Taq II mix (Takara, Shiga, Japan). mRNA expression levels were corrected using endogenous *GAPDH* as an internal control.

ELISA

Passage 2 hESCs cultured for 48 h were centrifuged and the supernatant was collected. ELISAs were performed using commercial ELISA kits (Quantikine ELISA kits, R&D Systems Inc., Minneapolis, MN, USA) according to the manufacturer's protocol for five cytokine and chemokine proteins belonging to the SASP: IL6, IL8 (encoded by *CXCL8*), IL17A, RANTES (encoded by *CCL5*), and MCP1 (encoded by *CCL2*). Absorbance was measured using a Model 680 Microplate Reader (Bio-Rad Laboratories Inc., Hercules, CA, USA) according to the instruction manual.

Western blotting

Passage 1 hESCs were harvested and lysed with cell lysis buffer (Merck KGaA, Darmstadt, Germany) with Protease Inhibitor Mixture (Nacalai Tesque, Kyoto, Japan) and phosphatase inhibitors (Nacalai Tesque). The cell lysates were separated on 10% SDS-polyacrylamide gels and transferred onto polyvinylidene difluoride membranes (Millipore, Billerica, MA, USA). The membrane was blocked by incubation with skim milk in 0.1% Tris-buffered saline with Tween 20 (TBST) for 90 min. Subsequently, the membrane was incubated overnight at 4 °C with primary antibodies. The primary antibodies used were anti-ERα (H-184) and -GAPDH (FL-335) (Santa Cruz Biotechnology, Santa Cruz, CA, USA) antibodies. The following day, the membrane was washed with TBST three times for 5 min each time. Subsequently, the membranes were incubated with a goat anti-rabbit horseradish peroxidase-conjugated secondary antibody (Sigma Aldrich) for 1 h at 37 °C, followed by treatment with Clarity Western ECL Substrate detection kits (Bio-Rad), and subjected to a ChemiDoc XRS Touch Imaging System (Bio-Rad). The intensities of the bands were quantified with Image Lab software (ver. 6.0; Bio-Rad) and were normalized against the bands obtained for GAPDH. MCF-7 cells were used as a positive control. All the antibodies used are listed in Supplemental Table S5.

Statistical analysis

The normality of the data was confirmed using the Kolmogorov–Smirnoff test. Normally distributed data were compared using an unpaired *t*-test with Welch correction. Non-normally distributed data were compared using a Mann–Whitney *U* test. Binary variables were compared using a Chi-square test. GraphPad Prism 5.0 software (GraphPad Inc., San Diego, CA, USA) was used for statistical analysis. Statistical significance was set at $P < 0.05$.

Results

Senescence rates based on SA-β-Gal staining

Cellular senescence was evaluated in terms of SA-β-Gal positivity among hESCs originating from receptive (n = 7) and non-receptive (n = 23) patients. No significant differences were observed between the two groups in terms of their background characteristics (Supplemental Table S6). SA-β-Gal-positive rates (%, mean ± SEM) on the 2nd, 4th, 6th, and 8th days of culture were as follows: receptive: 23.0 ± 6.8, 24.0 ± 10.7, 27.7 ± 10.3, 30.0 ± 11.5; non-receptive: 35.5 ± 16.1, 27.7 ± 13.6, 28.7 ± 14.8, 33.8 ± 10.3 (Figure 1). Senescent hESCs occupied a significantly higher proportion of non-receptive samples after 2 days of culture ($P < 0.01$).

Cell cycle analysis

Cell cycle analysis was performed on hESCs originating from receptive (n = 7) and non-receptive (n = 15) patients. No significant differences were observed between the two groups in terms of their background characteristics (Supplemental Table S7). Respective proportions of hESCs in the G0/G1, S, and G2/M phases (%, mean ± SEM) were as follows: receptive: 65.6 ± 8.2, 24.8 ± 4.1, 9.6 ± 9.0; non-receptive: 75.4 ± 7.1, 16.6 ± 6.5, 8.1 ± 2.6 (Figure 2). G0/G1 cells occupied a significantly greater proportion of non-receptive samples compared with receptive samples ($P < 0.01$), suggesting marked cell cycle arrest. In addition, the non-receptive group had a significantly lower percentage of S-phase cells ($P < 0.01$).

SA gene expression levels

Quantitative RT-PCR was used to compare the expression levels of three SA genes—*CDKN2A*, *CDKN1A*, and *TP53*—in hESCs originating from receptive (n = 10) and non-receptive (n = 21) patients. No significant differences were observed between the two groups in terms of their background characteristics (Supplemental Table S8). *CDKN2A* and *CDKN1A* expressions were significantly higher in non-receptive samples compared with receptive samples ($P < 0.05$; Figure 3).

SASP gene and protein expression levels

ELISA was used to quantify the expressions of five cytokine and chemokine proteins belonging to the SASP—IL6, IL8, IL17A, RANTES, and MCP1—in supernatants from hESC cultures originating from receptive (n = 9) and non-receptive (n = 26) patients. No significant differences were observed between the two groups in terms of their background characteristics (Supplemental Table S9). Expressions of all cytokines and chemokines were higher in non-receptive samples compared with receptive samples, although these trends were nonsignificant (Figure 4).

Quantitative RT-PCR was used to compare the expressions of four genes encoding SASP cytokines and chemokines—*IL6*, *CXCL8*, *IL17A*, and *CCL2*—in hESCs originating from receptive (n = 10) and non-receptive (n = 21) patients. No significant differences were observed between the two groups in terms of their background characteristics (Supplemental Table S8). All gene expressions were significantly higher in non-receptive samples compared with receptive samples ($P < 0.001$; Figure 5).

Somatic stem cell-related gene expression levels

Quantitative RT-PCR was used to compare the expressions of two genes highly expressed in somatic stem cells—*ABCG2* and *ALDH1A1*—in hESCs originating from receptive (n = 10) and non-receptive (n = 21) patients. No significant differences were observed between the two groups in terms of their background characteristics (Supplemental Table S8) and ERα (Supplemental Figure S3). *ABCG2* and *ALDH1A1* expression were significantly lower in non-receptive samples compared with receptive samples ($P < 0.01$; Figure 6), indicating reduced numbers of endometrial stem cells.

Discussion

In this study, we examined whether the expressions of senescence and stem cell marker genes and proteins in hESCs isolated from

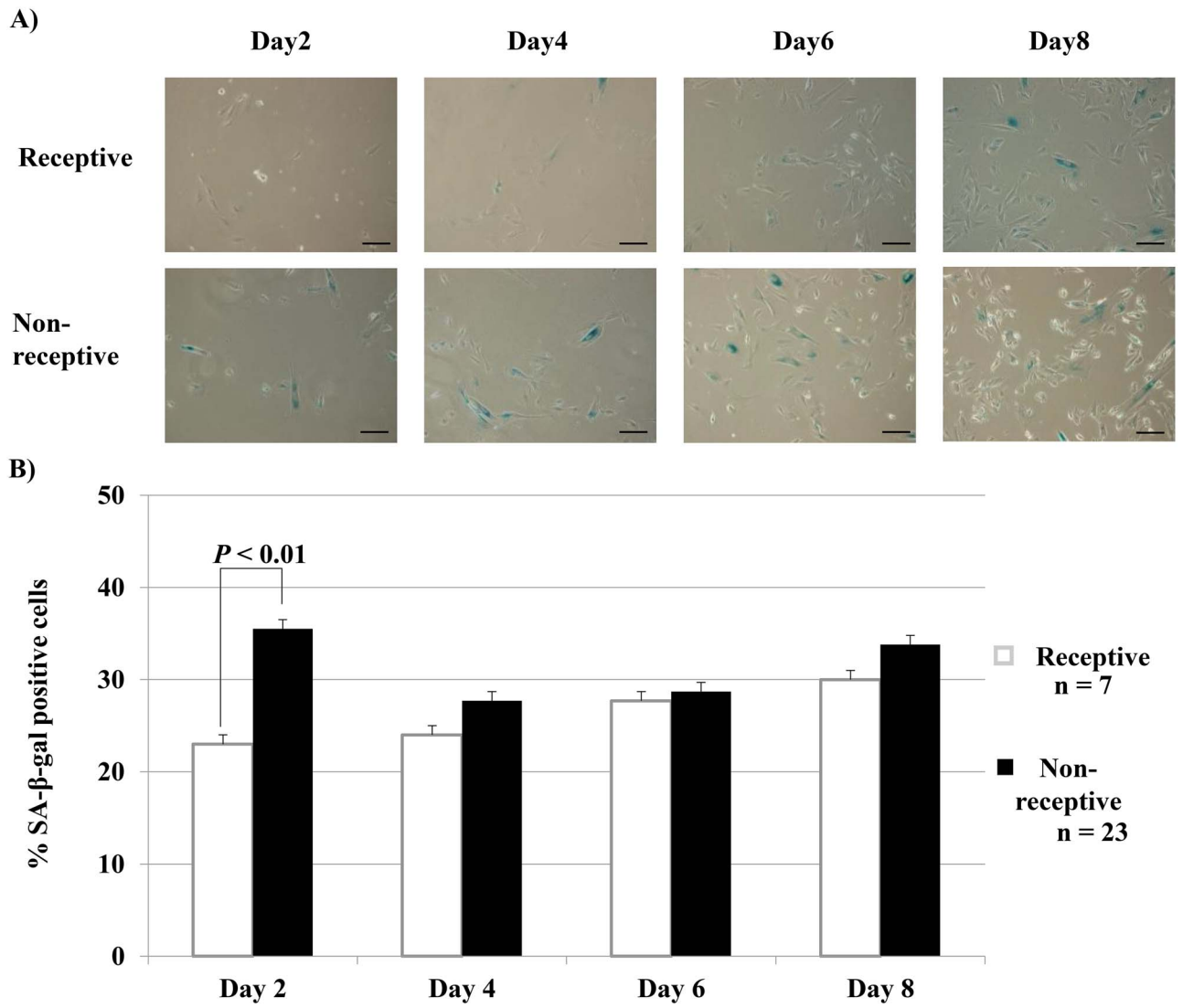

Figure 1. SA-β-Gal staining analysis of hESCs. (A) hESC cultures were inoculated on a 35-mm dish and then stained with SA-β-Gal every 48 h (Days 2, 4, 6, 8). Senescent cells appear blue. Scale bar = 100 μm. (B) Total cells and blue-stained cells were counted. Senescence rate was assessed as the ratio of SA-β-Gal-positive cells to total cells. All data represents mean ± SEM. The two groups are compared by an unpaired *t*-test with Welch correction.

endometrium sampled during the proliferative phase of the menstrual cycle were associated with cellular senescence induction and implantation failure among women receiving infertility treatment. Our intention was to look at the mechanism of implantation failure from a new perspective: that disruptions to local stem cell maintenance processes and microenvironment (niche) may play a role in stem cell decline, cellular senescence, and suppression of endometrial infiltration by trophoblasts.

First, we determined the proportions of senescent (SA-β-Gal-positive) hESCs originating from women who later successfully conceived and those who did not. We found a marked induction of cellular senescence in non-receptive patients at the earliest time point of in vitro culture (Day 2). Statistical significance was not observed from Day 4 as healthy cells replicated and diluted the relative proportion of senescent cells. Nonetheless, SA-β-Gal positivity rates were still higher in non-receptive patients in absolute terms compared with receptive samples. Thus, senescence seems to be excessively promoted in hESCs in non-receptive women, or alternatively, their senescence evasion mechanism is disrupted in some way. Telomere shortening induces senescence by limiting the replicative lifespan of normal somatic cells in repeated in vitro subcultures [21]. However, because we used first-generation hESCs, it seems more likely that cellular senescence observed in non-receptive women was stress-induced, attributable to oxidative stress or DNA damage [22], rather than restricted replication. Our cell cycle analysis findings corroborate this hypothesis. One hallmark of stress-induced senescence is the irreversible arrest of cell proliferation, halting affected cells in G0/G1. While many hESCs originating from receptive patients were in the S phase, indicating active replication, relatively few originated from non-receptive women; instead, G0/G1 cells were overrepresented, suggesting high numbers of senescent cells in cell cycle arrest. Several signaling pathways, notably p53/p21 and p16/RB, have been implicated in cellular aging at the molecular level [23]. Here, we investigated the relative expression of three genes associated with cellular senescence: *CDKN2A*, *CDKN1A*, and *TP53*, which respectively encode p16, p21, and p53. *CDKN1A* and *CDKN2A*

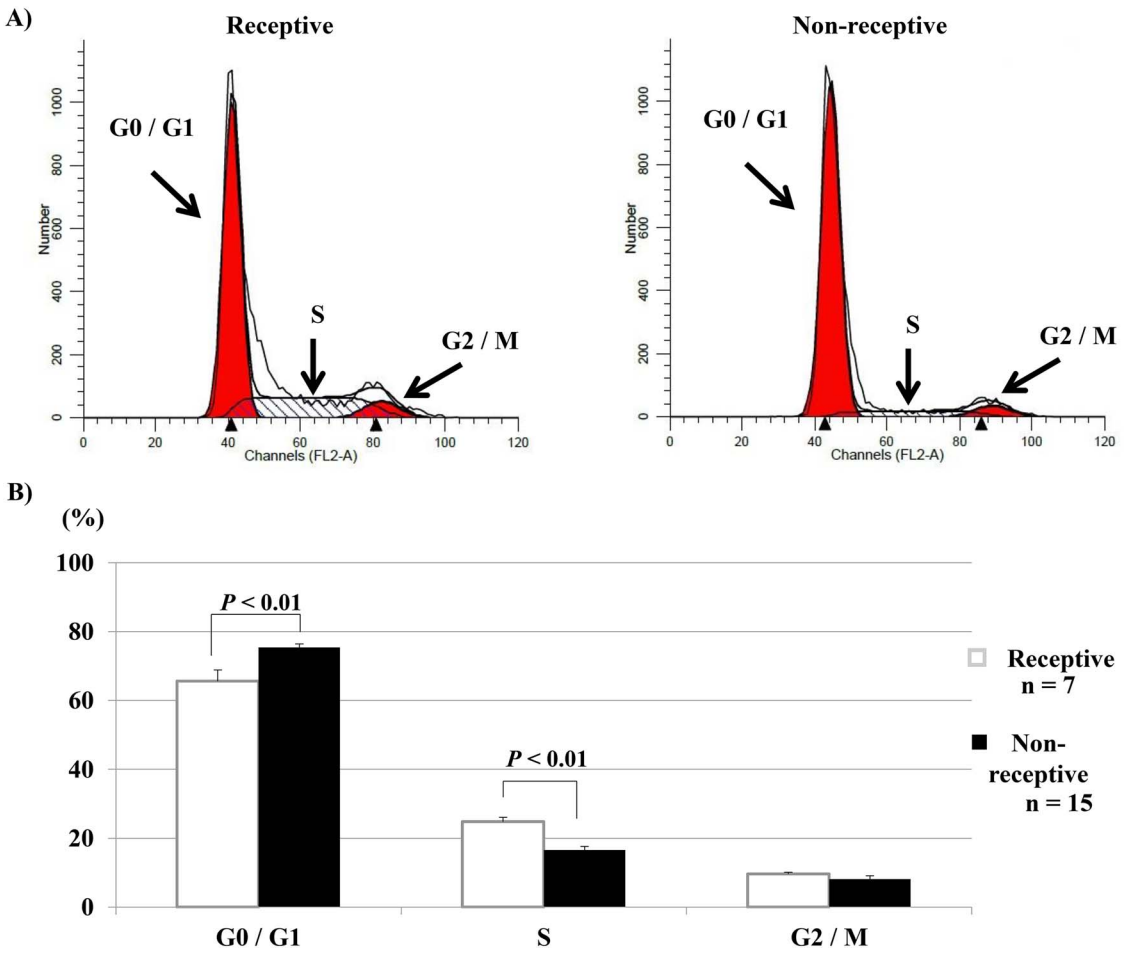

Figure 2. Cell cycle analysis of hESCs. (A) hESCs were cultured for 8 days, and then subjected to cell cycle analysis. DNA content was measured for at least 20 000 cells for each sample. Representative data are shown. (B) Proportions of hESCs in G0/G1, S, and G2/M were calculated. All data represents mean ± SEM. The two groups are compared by an unpaired *t*-test with Welch correction.

expressions were elevated in hESCs originating from non-receptive patients, corroborating the trends observed in SA-β-Gal staining and cell cycle analysis. This implicates p21- and p16-mediated signaling pathways (and probably others) in the induction of senescence in this cell type. We inferred a putative mechanism as follows. During normal cell division, cyclins and cyclin-dependent kinases (CDKs) phosphorylate retinoblastoma protein (Rb) to release bound E2F proteins, a family of transcription factors crucial for the G1/S transition. p21 and p16 are members of the CDK inhibitor (CDKI) family, which bind to and inactivate these cyclins and CDKs. Consequently, E2F proteins remain permanently bound to Rb, arresting the cell cycle and inducing senescence [22]. There are two potential reasons why we observed no difference in *TP53* expression between receptive and non-receptive patients. First, while p21 expression is often promoted by p53, it does not necessarily need to be: Putative p53-independent upstream factors include the mitogen-activated protein kinase (MAPK) p38, as well as c-Jun N-terminal kinase (JNK) cascades. However, histone deacetylase (HDAC) inhibitors upregulated p21 independently of p53 and inhibited proliferation in colon cancer cells lacking the p53 promoter [24]. Thus, senescent cells may have less acetylation at the p21 promoter region compared with healthy cells, thus upregulating p21 transcription independently of the p53/p21 pathway. Moreover, each of these signaling pathways is activated by environmental stressors such as DNA damage, oxidation, high osmotic pressure, heat shock, and inflammatory cytokines such as tumor necrosis factor (TNF) and interleukins (e.g., IL-1). Therefore, cellular senescence in non-receptive women may be attributable to exposure to severe microenvironmental stress.

Although cell cycle arrest is a hallmark of senescent cells, recent research has revealed that they secrete a variety of physiologically active molecules such as inflammatory cytokines, chemokines, growth factors, and matrix metalloproteinases [25, 26]. This phenomenon has been termed the SASP or, alternatively, the senescence messaging secretome (SMS) [27, 28]. Here, we compared the expression levels of several SASP-related cytokines and chemokines—IL6, IL8, IL17A, RANTES, and MCP1—in hESC culture supernatant as well as those of SASP-related genes: *IL6*, *CXCL8*, *IL17A*, and *CCL2*. While we observed no differences in protein expressions associated with implantation failure, all surveyed genes were more highly expressed in samples originating from non-receptive patients than receptive patients. The discrepancies between the results of protein expression and mRNA levels are attributed to differences in the analyzed materials. In other words, gene expression was analyzed by extracting total RNA from cells, while protein expression was analyzed by culture supernatant. It is possible that a limited number of cell cultures was not a sufficient condition for comparing protein expression. Much remains unclear about the local effects of these SASP factors. They were reported to influence the tissue microenvironment by multiple pathways, including promoting and inhibiting tumor formation, inducing apoptosis, triggering

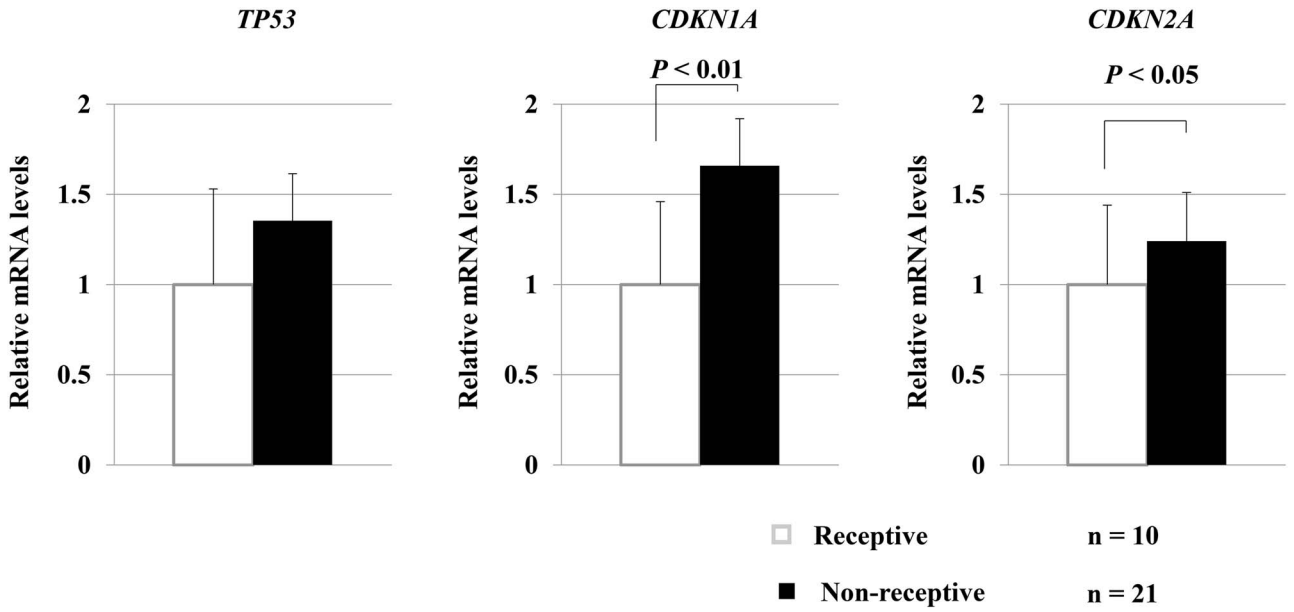

Figure 3. Relative quantitative analysis of SA genes in hESCs. qRT-PCR was used to quantify relative mRNA transcript levels of the SA genes *CDKN2A* (p16), *CDKN1A* (p21), and *TP53* (p53) in primary hESCs. All values are corrected with respect to an internal standard (*GAPDH* mRNA). All data represents mean ± SEM. The two groups are compared by an unpaired *t*-test with Welch correction.

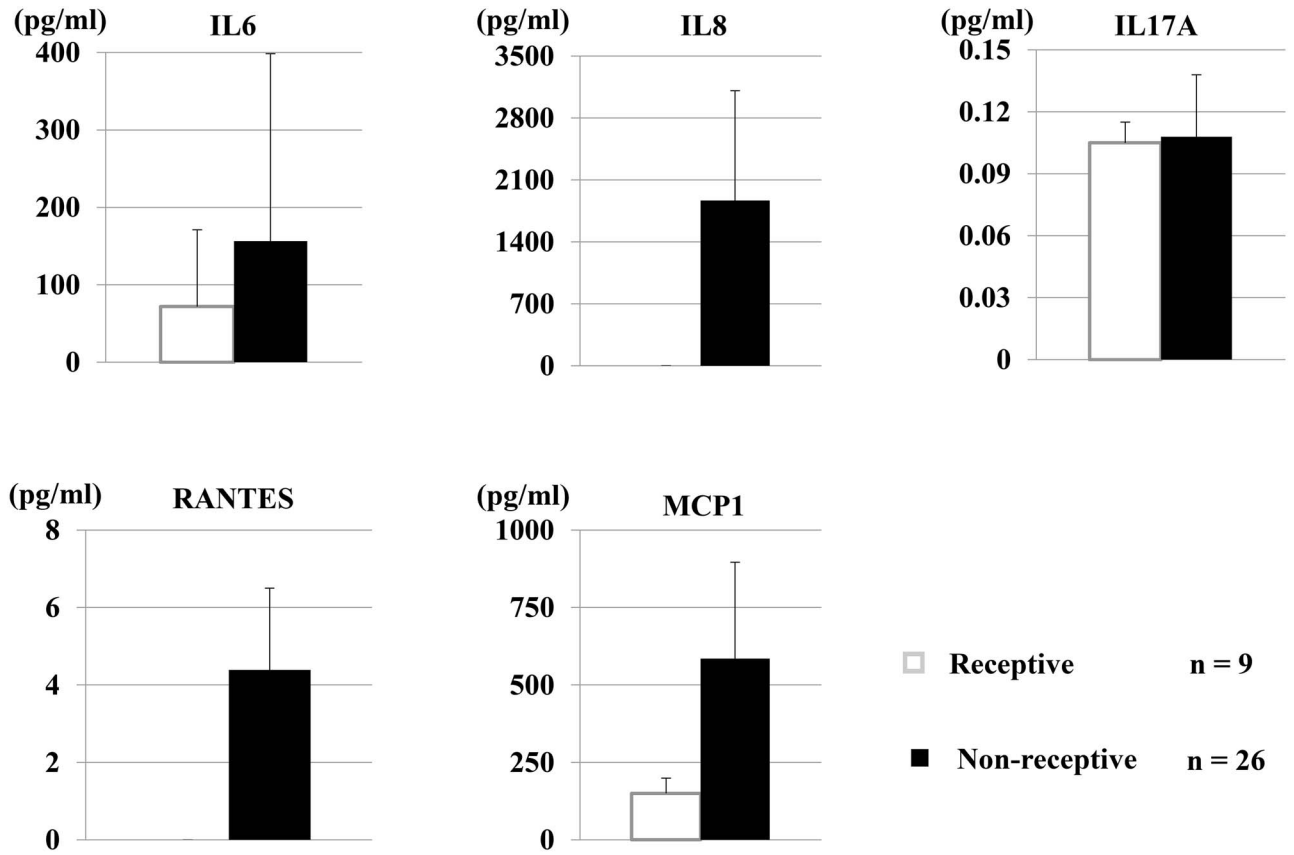

Figure 4. Quantitative analysis of SASP cytokines/chemokines in hESCs. ELISA was used to quantify levels of five SASP cytokines/chemokines (IL6, IL8, IL17A, RANTES, and MCP1) in supernatants of hESCs cultured for 48 h. All data represents mean ± SEM. No significant differences were observed between the two groups. The two groups are compared by a Mann–Whitney *U* test.

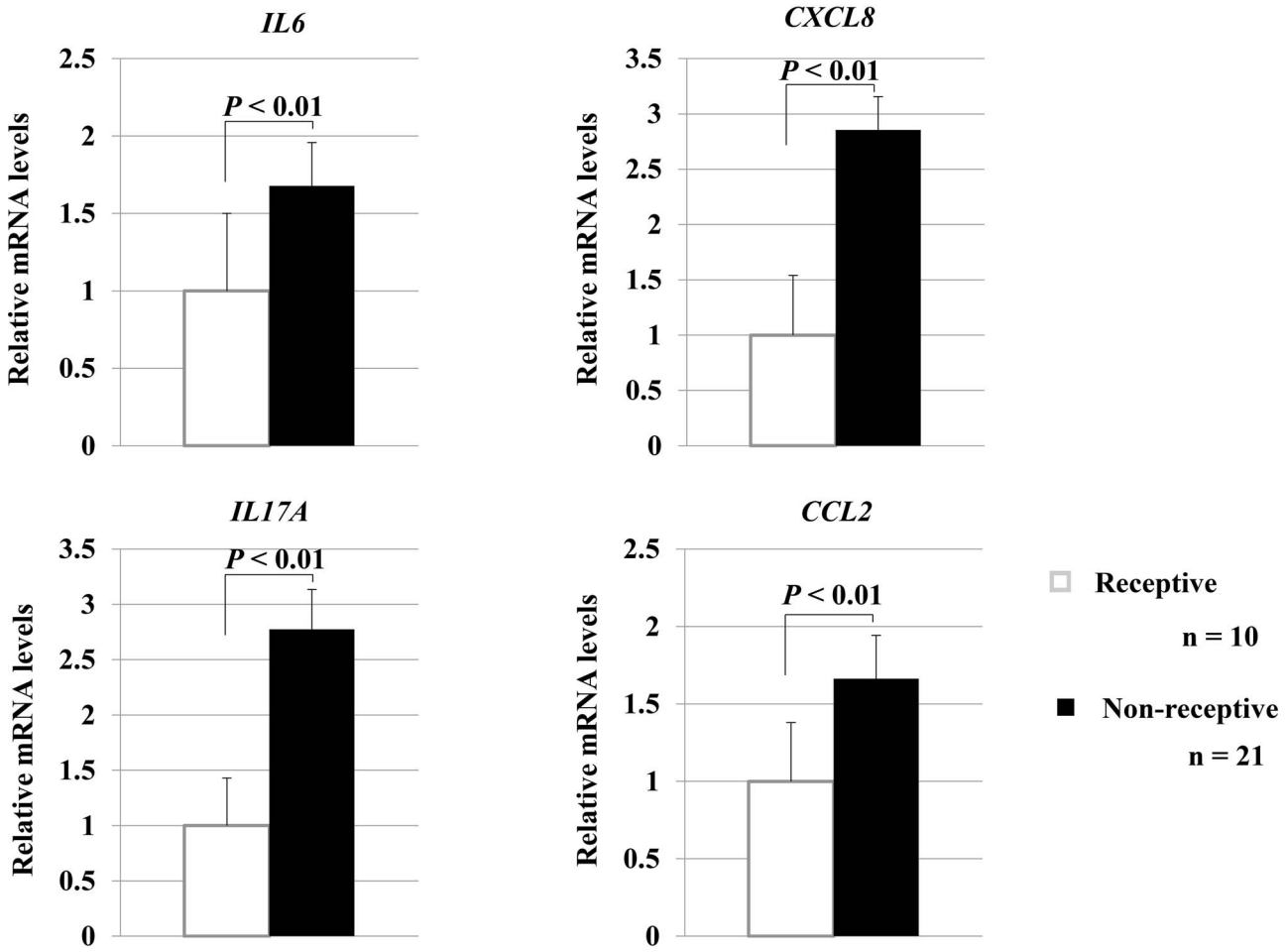

Figure 5. Relative quantitative analysis of SASP genes in hESCs. qRT-PCR was used to quantify relative mRNA transcript levels of four genes encoding SASP proteins (*IL6*, *CXCL8*, *IL17A*, and *CCL2*) in hESCs. All values are corrected with respect to an internal standard (*GAPDH* mRNA). All data represents mean ± SEM. The two groups are compared by an unpaired *t*-test with Welch correction.

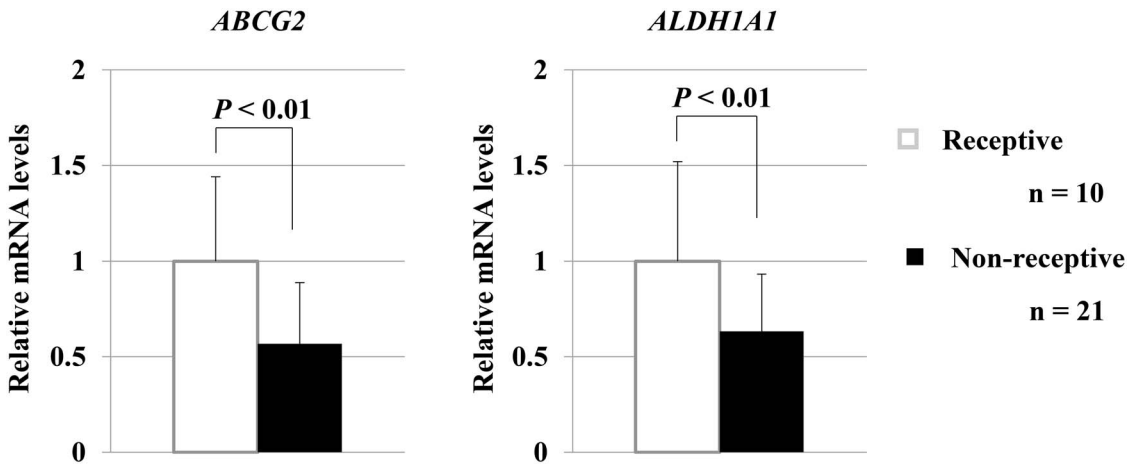

Figure 6. Relative quantitative analysis of somatic stem cell-related genes in hESCs. qRT-PCR was used to quantify relative mRNA transcript levels of two genes highly expressed in somatic stem cells (*ABCG2* and *ALDH1A1*) in hESCs. All values are corrected with respect to an internal standard (*GAPDH* mRNA). All data represents mean ± SEM. The two groups are compared by an unpaired *t*-test with Welch correction.

inflammation, accelerating senescence, and epigenetic suppression, via autocrine and paracrine mechanisms [29–32]. However, no research has reported their effects on endometrial receptivity. Our novel observations of the elevated expression of all SASP genes assayed implicate these factors in reduced embryonic receptivity during the proliferative phase of the menstrual cycle. Hereafter, we plan to investigate the effects of SASP factors on endometrial somatic and stem cells, as well as embryonic developmental potential and trophoblast cell function (including the epithelial–mesenchymal transition).

Cellular senescence reportedly plays a critical role in hESC decidualization and embryo implantation [33]. Kuroda and colleagues' showed that the retinoic acid signaling pathway, important in decidualization, activated both differentiation- and senescence-inducing factors. The SA-β-Gal staining rate was increased among decidualizing endometrial cells with time, and suppressing senescence induction inhibited decidualization and prevented embryo implantation. Taken together, their findings imply that implantation crucially depends on a balance between cellular differentiation and senescence during endometrial decidualization [7–9]. Brighton et al. [34] also reported that the transcription factor Forkhead box O1 induced cellular senescence in decidualizing hESCs that was IL-8 dependent. However, the influence of endometrial cellular senescence on the proliferative phase before decidualization on embryo implantation is unknown. Our findings suggest the induction of cellular senescence in hESCs during the proliferative phase of the menstrual cycle negatively affects embryo implantation. In the future, we plan to investigate how senescence induced during the proliferative phase affects the subsequent decidualization process, as well as trophoblast infiltration.

Somatic stem cell populations become depleted as organisms advance in age, and senescence-related pathways are triggered more frequently at the cellular level [35]. Here, we investigated the expression levels of two genes in hESCs: *ABCG2*, a stem cell marker strongly expressed in SP cells, and *ALDH1A1*, a mesenchymal stem cell marker. In addition to enhanced senescence as mentioned above, non-receptive patients exhibited lower expressions of both genes than their counterparts who later became pregnant. Thus, cellular senescence appears to be associated with a loss of stemness among hESC populations. Several mechanisms are plausible: Senescence might be caused by disruptions to stemness maintenance pathways or, conversely, trigger the release of factors into the tissue microenvironment (niche) that cause stem cells to lose their characteristic properties. While the causality is uncertain, our findings suggest that enhanced senescence is associated with reduced numbers of stem cells in endometrial tissues and implicate these two phenomena in the pathology of implantation failure in infertility patients.

In summary, a wide variety of biological markers of cellular senescence were markedly enhanced in hESCs originating from infertility patients whose embryo transfers did not result in a pregnancy, compared with their successful counterparts of a similar age and background. These patients also exhibited lower levels of mRNA transcripts for *ABCG2* and *ALDH1A1*, two markers of somatic stem cells, suggesting depletion of the stem cell population in their endometrial tissue. Taken together, our findings constitute a novel contribution to the literature, suggesting that stemness maintenance is inversely associated with senescence induction in hESCs and, by extension, that implantation failure during infertility treatment may be attributable to a combination of senescence promotion and disruption of this maintenance function in this population during the proliferative phase of the menstrual cycle. However, it is known that cellular senescence and implantation failure in infertile patients are caused by aging. In this study, age and the levels of E2 and ERα were not significantly different between the two groups, but age-stratified analysis may be necessary in the future. This study was limited by the small numbers in each group. In addition, we should note that poor embryo quality may have been responsible for some cases of implantation failure in our non-receptive patients: thus, our non-receptive group may have included some women with normal endometrium. PGT-A would have enabled us to check, but this procedure is not allowed in Japan. Future work should consider how PGT-A or similar means could be incorporated to eliminate poor-quality embryos. Moreover, the specific mechanism by which implantation failure is prefigured by a loss of stemness among endometrial stem cells, and cellular senescence induction among hESCs should be elucidated in detail.

Supplementary material

Supplementary material is available at *BIOLRE* online.

Author contributions

HT designed the study, performed experiments, acquired and interpreted data and wrote the manuscript. TK, KA, KE, KK, KH, and YN assisted in acquiring and interpreting data. KK designed the study, interpreted data, and wrote the manuscript. All authors reviewed the manuscript and accepted the final version.

Acknowledgments

We appreciate Ms. Adachi and Research Support Center, Graduate of Medical Science, Kyushu University for excellent technical support. We are also immensely grateful to the staff and patients at IVF Nagata Clinic for the provision of tissue samples for our research.

Conflict of interest

The authors declare no conflict of interests.

References

1. Baird DT, Collins J, Egozcue J, Evers LH, Gianaroli L, Leridon H, Sunde A, Templeton A, van Steirteghem A, Cohen J, Crosignani PG, Devroey P et al. ESHRE Capri workshop group. Fertility and ageing. *Hum Reprod Update* 2005; **11**:261–276.
2. Harton GL, Munne S, Surrey M, Grifo J, Kaplan B, McCulloh DH, Griffin DK, Wells D. Diminished effect of maternal age on implantation after preimplantation genetic diagnosis with array comparative genomic hybridization. *Fertil Steril* 2013; **100**:1695–1703.
3. Forman EJ, Tao X, Ferry KM, Taylor D, Treff NR, Scott RT Jr. Single embryo transfer with comprehensive chromosome screening results in improved ongoing pregnancy rates and decreased miscarriage rates. *Hum Reprod* 2012; **27**:1217–1222.
4. Keltz MD, Vega M, Sirota I, Lederman M, Moshier EL, Gonzales E, Stein D. Preimplantation genetic screening (PGS) with comparative genomic hybridization (CGH) following day 3 single cell blastomere biopsy markedly improves IVF outcomes while lowering multiple pregnancies and miscarriages. *J Assist Reprod Genet* 2013; **30**:1333–1339.
5. Lim HJ, Wang H. Uterine disorders and pregnancy complications: Insights from mouse models. *J Clin Invest* 2010; **120**:1004–1015.
6. Brosens JJ, Salker MS, Teklenburg G, Nautiyal J, Salter S, Lucas ES, Steel JH, Christian M, Chan YW, Boomsma CM, Moore JD, Hartshorne GM

et al. Uterine selection of human embryos at implantation. *Sci Rep* 2014; **4**:3894.
7. Kuroda K, Venkatakrishnan R, Salker MS, Lucas ES, Shaheen F, Kuroda M, Blanks A, Christian M, Quenby S, Brosens JJ. Induction of 11β-HSD 1 and activation of distinct mineralocorticoid receptor- and glucocorticoid receptor-dependent gene networks in decidualizing human endometrial stromal cells. *Mol Endocrinol* 2013; **27**:192–202.
8. Kuroda K, Venkatakrishnan R, James S, Sucurovic S, Mulac-Jericevic B, Lucas ES, Takeda S, Shmygol A, Brosens JJ, Quenby S. Elevated preimplantation uterine natural killer cell density in human endometrium is associated with impaired corticosteroid signaling in decidualizing stromal cells. *J Clin Endocrinol Metab* 2013; **98**:4429–4437.
9. Ozaki R, Kuroda K, Ikemoto Y, Ochiai A, Matsumoto A, Kumakiri J, Kitade M, Itakura A, Muter J, Brosens JJ, Takeda S. Reprogramming of the retinoic acid pathway in decidualizing human endometrial stromal cells. *PLoS One* 2017; **12**:e0173035.
10. Matsumoto H, Ma WG, Daikoku T, Zhao X, Paria BC, Das SK, Trzaskos JM, Dey SK. Cyclooxygenase-2 differentially directs uterine angiogenesis during implantation in mice. *J Biol Chem* 2002; **277**:29260–29267.
11. Menkhorst E, Salamonsen L, Robb L, Dimitriadis E. IL11 antagonist inhibits uterine stromal differentiation, causing pregnancy failure in mice. *Biol Reprod* 2009; **80**:920–927.
12. Ruiz-Alonso M, Blesa D, Diaz-Gimeno P, Gomez E, Fernandez-Sanchez M, Carranza F, Carrera J, Vilella F, Pellicer A, Simon C. The endometrial receptivity array for diagnosis and personalized embryo transfer as a treatment for patients with repeated implantation failure. *Fertil Steril* 2013; **100**:818–824.
13. Kato K, Yoshimoto M, Kato K, Adachi S, Yamayoshi A, Arima T, Asanoma K, Kyo S, Nakahata T, Wake N. Characterization of side-population cells in human normal endometrium. *Hum Reprod* 2007; **22**:1214–1223.
14. Kato K, Kusunoki S, Inagaki T, Yusuf N, Suga S, Terao Y, Arima T, Tsukimori K, Takeda S. Side-population cells derived from non-tumorigenic rat endometrial cells are a candidate cell of origin for malignant endometrial tumors. *J Stem Cell Res Ther* 2012. doi: 10.4172/2157-7633.S7-003.
15. Kato K, Horiuchi S, Takahashi A, Ueoka Y, Arima T, Matsuda T, Kato H, Nishida J, Nakabeppu Y, Wake N. Contribution of estrogen receptor alpha to oncogenic K-Ras-mediated NIH3T3 cell transformation and its implication for escape from senescence by modulating the p53 pathway. *J Biol Chem* 2002; **277**:11217–11224.
16. Tomari H, Honjou K, Nagata Y, Horiuchi T. Relationship between meiotic spindle characteristics in human oocytes and the timing of the first zygotic cleavage after intracytoplasmic sperm injection. *J Assist Reprod Genet* 2011; **28**:1099–1104.
17. Tomari H, Honjo K, Kunitake K, Aramaki N, Kuhara S, Hidaka N, Nishimura K, Nagata Y, Horiuchi T. Meiotic spindle size is a strong indicator of human oocyte quality. *Reprod Med Biol* 2018; **17**: 268–274.
18. Satyaswaroop PG, Bressler RS, de la Pena MM, Gurpide E. Isolation and culture of human endometrial glands. *J Clin Endocrinol Metab* 1979; **48**:639–641.
19. Seli E, Senturk L, Bahtiyar OM, Kayisli UA, Arici A. Expression of aminopeptidase N in human endometrium and regulation of its activity by estrogen. *Fertil Steril* 2001; **75**:1172–1176.
20. Livak KJ, Schmittgen TD. Analysis of relative gene expression data using real-time quantitative PCR and the 2-$\Delta\Delta$CT method. *Methods* 2001; **25**:402–408.
21. Hayflick L, Moorhead PS. The serial cultivation of human diploid cell strains. *Exp Cell Res* 1961; **25**:585–621.
22. Campisi J, d'Adda di Fagagna F. Cellular senescence: When bad things happen to good cells. *Nat Rev Mol Cell Biol* 2007; **8**:729–740.
23. Gorospe M, Abdelmohsen K. MicroRegulators come of age in senescence. *Trends Genet* 2011; **27**:233–241.
24. Archer SY, Meng S, Shei A, Hodin RA. p21 (WAF1) is required for butyrate-mediated growth inhibition of human colon cancer cells. *Proc Natl Acad Sci U S A* 1998; **95**:6791–6796.
25. Coppe JP, Patil CK, Rodier F, Sun Y, Munoz DP, Goldstein J, Nelson PS, Desprez PY, Campisi J. Senescence-associated secretory phenotypes reveal cell-nonautonomous functions of oncogenic RAS and the p53 tumor suppressor. *PLoS Biol* 2008; **6**:2853–2868.
26. Campisi J, Andersen JK, Kapahi P, Melov S. Cellular senescence: A link between cancer and age-related degenerative disease? *Semin Cancer Biol* 2011; **21**:354–359.
27. Campisi J. Aging, cellular senescence, and cancer. *Annu Rev Physiol* 2013; **75**:685–705.
28. Kuilman T, Peeper DS. Senescence-messaging secretome: SMS-ing cellular stress. *Nat Rev Cancer* 2009; **9**:81–94.
29. Wajapeyee N, Serra RW, Zhu X, Mahalingam M, Green MR. Oncogenic BRAF induce senescence and apoptosis through pathways mediated by the secreted protein IGFBP7. *Cell* 2008; **132**:363–374.
30. Acosta JC, Banito A, Wuestefeld T, Georgilis A, Janich P, Morton JP, Athineos D, Kang TW, Lasitschka F, Andrulis M, Pascual G, Morris KJ et al. A complex secretory program orchestrated by the inflammasome controls paracrine senescence. *Nat Cell Biol* 2013; **15**:978–990.
31. Takahashi A, Imai Y, Yamakoshi K, Kuninaka S, Ohtani N, Yoshimoto S, Hori S, Tachibana M, Anderton E, Takeuchi E, Shinkai Y, Peters G et al. DNA damage signaling triggers degradation of histone methyltransferases through APC/C(Cdh1) in senescent cells. *Mol Cell* 2012; **45**:123–131.
32. Vassilieva IO, Reshetnikova GF, Shatrova AN, Tsupkina NV, Kharchenko MV, Alekseenko LL, Nikolsky NN, Burova EB. Senescence-messaging secretome factors trigger premature senescence in human endometrium-derived stem cells. *Biochem Biophys Res Commun* 2018; **496**:1162–1168.
33. Leno-Duran E, Ruiz-Magana MJ, Munoz-Femandez R, Requena F, Olivares EG, Ruiz-Ruiz C. Human decidual stromal cells secrete soluble pro-apoptotic factors during decidualization in a cAMP-dependent manner. *Hum Reprod* 2014; **29**:2269–2277.
34. Brighton PJ, Maruyama Y, Fishwick K, Vrljicak P, Tewary S, Fujihara R, Muter J, Lucas ES, Yamada T, Woods L, Lucciola R, Hou Lee Y et al. Clearance of senescent decidual cells by uterine natural killer cells cycling human endometrium. *elife* 2017; **6**:e31274.
35. Collado M, Blasco MA, Serrano M. Cellular senescence in cancer and aging. *Cell* 2007; **130**:223–233.